STAR Note 227

Simulation results and suggestions for possible design of gaseous shower maximum detector for the EMC Endcap

G.Averichev, S.Chernenko, E.Matyushevskiy, Yu.Minaev, Yu. Panebratsev, E.Potrebenikova, D. Razin, S.Razin, L.Smykov, G.Škoro, A.Shabunov, I.Tsvetkov, V.Yurevich, Yu.Zanevskiy

**Laboratory of High Energy Physics,
Joint Institute for Nuclear Research,
141980 Dubna, Russia**

November 9, 1995

Abstract

The Monte Carlo simulation of Shower Maximum Detector (SMD) for the Endcap EMC has been performed for **pp**, **pAu** and **AuAu** collisions. A conceptual design of gaseous SMD with a pad readout of signals is proposed.

1 Introduction

In our previuos note (**STAR Note 226**) we presented the results of Monte Carlo simulations of Endcap EMC Shower Maximum Detector (**SMD**) for the STAR and experimental investigations of characteristics of the russian tiny photomultipliers **PMT** in order to specify their applicability in the **SMD**. Our results show that the scintillator strip/fiber **SMD** is good option for the Endcap **SMD** in the case of **pp** and **pAu** collisions. Application of russian tiny **PMT** with low gain allows us to build relatively low-cost **SMD** with low number of high voltage supply channels. But, one of the most important conclusions of our previous work [1] was that this type **SMD** is not suited for the job in the **AuAu** collision case. In what follows, we present results of our MC calculations and main ideas about the conceptual design of **SMD** for EMC Endcap with a pad readout of signals.

2 Monte Carlo simulations

2.1 SMD parameters

The CERN Monte Carlo program GEANT3.15 with a 1 MeV cut for γ's and electrons was used to study EM showers for full STAR detector and HIJING model event generator has been used for describing of proton-nucleus and nucleus-nucleus collisions.

During the MC simulations the **SMD** was placed at the depth of $5X_o$ in the endcap EMC and consisted of two scintillation rings (inner radius – 75 cm, outer radius – 232 cm, thickness – 6 mm).

In **Fig.1** the pseudorapidity distributions of γ's and charged hadrons in **pp**, **pAu** and **AuAu** collisions are presented. The distributions of energies for direct gammas and gammas from π^o decays in acceptance of the endcap EMC are shown in the right side of this picture. The number of γ's in the **SMD** acceptance is about 800 for central **AuAu** collision and about 10 in central **pAu** collision.

Scatter plot of shower charged particles distribution on the first **SMD** layer is presented in **Fig.2a**. In **Fig.2b** we show the number of this particles as a function of the distance **R** from the **SMD** centre. It is seen that about 75% of showers, produced in the interactions of primary γ's (about 600) with the calorimeter matter, lie in the central ($75 < R < 160$ cm) **SMD** region.

The same distributions for the primary gammas with energy above 500 MeV are presented in **Fig.3**. Comparison of **Fig.2** and **Fig.3** tells us that the contribution of showers, induced by gammas with energy lower then 500 MeV, is practically negligible, and we can conclude that the main sources of background (for observation of direct γ's) are hadrons and gammas with energy higher than 500 MeV.

Fig.4 shows the transverse profiles of shower, induced by 15 GeV gamma on the middle part of the first and second layer of **SMD** at the pseudorapidity $\eta \simeq 1.5$. RMS of the shower transverse profiles is about 2.3 cm. This means that the granularity of the **SMD** must be better then 10-12 mm for both layers in order to identify and separate the showers. The IHEP group experimental data [2] confirm our conclusion.

To obtain a uniform deposited energy over full surface of **SMD** layer, we have account for dependence of deposited energy on the radius **R** in the central **SMD** region ($75 < R < 160$) cm. We can see that for $R > 160$ cm deposited energy practically does not depend on the distance **R**. The data for the central **SMD** region were used for the fitting procedure and the fitted function was of the form $\Delta E = a + b \cdot R$. The results of the fit were used to determine the width of the inner ring strips, taking into accout that the widths of outer strips are equal $\Delta R = 12$ mm. The total number of ring strips defined in such manner is 190. The total width of the central ring strip is 4 mm.

The next step was a determination of a number of strips in the azimuthal direction and, as a result we have practically defined the pad stucture of the **SMD** layer. In **Fig.5** is shown the energy deposited in the central 6 cm width ring of **SMD** vs. azimuthal angle for 6^o, 3^o and 1^o per bin for the central **AuAu** collision. The width of 6 cm corresponds to the full width at 1/10 th of maximum height of the shower transverse profile. The 1^o azimuthal angle bin corresponds to the geometrical size of ~ 13 mm in the central part of **SMD** and using these pads we can clearly identify the single shower. Refering to the **Fig.5a** and **Fig.5b** it is seen that all showers are separated with the 3^o azimuthal angle widths pads. Finally, the proposed pad structure of the first **SMD** plane gives us the possibility to separate showers in the central **SMD** region using the information about two coordinates (**R** and ϕ). But we would like to point out that for separating the showers in the outer part of the **SMD** the information about ϕ coordinate from the second plane (wires or strip with 10 mm step, for example) is needed.

2.2 π^o/γ separation

We have, also, carried out a study of the separation of shower coming from single γ from those coming from a π^o decay. In our calculation we considered a **SMD** with only one sensitive plane with the pad structure, described above. We used a procedure similar to the method, described in [3]. Three variables were used to find a coefficient of π^o rejection for 90 % γ acceptance:

- **E** – the energy deposited by the shower;
- **r** – the energy weighted shower radius;
- $\mathbf{Er^2}$ - the energy dispersion of the shower.

The energy weighted center of the shower is calculated as follows:

$$X_c = \sum_i x_i E_i / \sum_i E_i$$

where E_i is the energy deposited in the *ith* pad and X_i is the position coordinate of the *ith* pad in the pad units. The energy weighted shower radius, **r** is calculated as:

$$r = \sum_i D_i E_i / \sum_i E_i$$

where $D =| X_c - X_i |$ is the distance of the *ith* pad from the calculated centre of the shower. The energy dispersion of the shower is calculated as:

$$Er^2 = \sum_i E_i D_i^2$$

Fig.6 shows the scatter plot of the energy dispersion Er^2 vs. the wighted shower radius **r** for 100 showers initiated by 15 GeV γ's and π^o's in the middle part of the **SMD** (rapidity $\eta \approx 1.5$). The energy summation was taken over 15 pads in radial and 10 in azimuthal directions from calculated center of the shower. The marked area in Fig.6a contains 90% of the single γ showers. In the scatter plot for π^o initiated showers the area of 90% single γ efficiency is marked. The showers within this area are classified as showers initiated by γ's, while all showers outside this area - as π^o initiated showers. The π^o rejection efficiency is given by the percentage of π^o initiated showers which are outside this area. In this case we have obtaned the π^o rejection efficiency of 63%. The results of the similar calculations for the **SMD** with two sensitive plans consisted of 1 cm width scintillator strips are shown in **Fig.7**. The value of the π^o rejection efficiency is 60% in this case. It is seen, that for the **SMD** with only one pad type sensitive plane we get practically the same π^o/γ separation as for the **SMD** with two strip type planes.

The future investigations are needed in this direction. In our opinion the information about the ϕ coordinate from second **SMD** plane will significantly improve the efficiency of π^o/γ separation.

3 Conceptual Design

Following by the Monte Carlo calculation results we propose to use as an option of **SMD** a thin multiwire gas chamber with analog readout of anode wires and of cathode pads to measure the position of EM showers. The analog readout is sensitive to the density of particles inside the shower, thus providing a localization of the shower core by a simple determination of the weighted centre in a cluster of signals. We adopt **OPAL** [4] and **CDF** [5] groups methods in our proposal. The thin multiwire gas chambers, operating in a satured mode, were used for electromagnetic presumpling in the endcaps of **OPAL** detector at **LEP** [4]. At Fermilab for the Collider Detector Faciliity the shower counter strip chamber were used operating with the gain of 10^4 [5].

The suggested **SMD** multiwire gas chamber will be **CDF** or **OPAL** type chamber with pad structure of cathode as followed from MC simulations.

3.1 Description of Detector

Space and timing restrictions are the major concern for detector design. It is proposed that the **SMD** will be inserted into 25 mm gap into the endcap EMC at the depth of $5 \div 7X_o$. It will consists of 12 trapezoidal sectors each of which covers of 30^o azimuthal angle. The geometrical dimensions are given in **Fig.8**. A schematic view of the cross section of two types chambers are shown in **Fig.9** and **Fig.10**.

In the **OPAL** type chamber (**Fig.9**) the anode wire plane consists of 637 gold coated tungsten W-Re wires of 30 μm diameter rounded on the supporting frame with space step of 2 mm in the direction along of the sector axes line. Groups of five wires are then **AND**ed. The wires strung with a tension of about $80 \div 100$ g. A long wires are supported every 60 cm by spacers to avoid sagging and to provide a mechanical strength for the chamber itself. The dead space loss due to this support is less than one percent.

The **CDF** type chamber (**Fig.10**) has a ribbed construction. Aluminum ribs profile will product using the extrusious technology. The anode wires are placed at the centre of cells with the step of 1 cm by means of a special supporting plates. The individual anode wire is connected to high voltage by 1 MΩ resistor and readout trough capacity of $200 \div 400$ pF.

The **IHEP** group has tested the strip prototype of multiwire gas chamber of **SMD** for barrel endcap EMC in May'95. We plan to co-operate with this group in manufacturing of aluminum ribs profile using russian industry.

The cathode planes of chambers are 1.5 mm thin G10 sheets of whose internal faces (forward wires) copper pads are formed by chemical etching. Following by the results of MC calculations there are 190 bins in radial and 10 bins in azimuthal directions, total – 1900 pads. The size of the pads decreases going towards the beam axes to resolve ambiguites due to increasing multiplicity. The cathode plane is placed at the distance of 3 mm from the anode wire plane.

The full cathode plane consists of a few pieces. These pieces are glued in turn to the face of G10 sheet to obtain the full cathode plane of the **SMD** sector. This cathode plane is glued to the ribs aluminum plate (**CDF** type chamber) or pressed to the supporting frame (**OPAL** type chamber). The outer face of cathode is used for readout electronics components. The gas mixture argon – DME or argon – CO_2 will be used.

3.2 Readout electronics

The two space coordinates are provided by the simultaneous readout of wire and pads. This results in a total 2027 electronic channels per sector and 24324 channels for full endcap **SMD**. All channels have multiplexing analog readout. The front end electronics is directly mounted onto outer face of the cathode plane. A shielded **TWP** cables is used to transport the signals to the rear end. At the rear end additional multiplexing will be obtained in the **ADC** module. 12 bit charge sensitive **ADC** will be enough to cover a dynamic range from minimum ionizing particles up to showers.

4 Conclusion

Our Monte Carlo calculation results show that the Shower Maximum Detector with pad structure of sensitive layer has more suitable properties than the corresponding strip type especially in the case of investigation of the EM showers in the **AuAu** collision. Good position resolution and π^o/γ shower separation are realised even with only one sensitive **SMD** layer used. The estimates indicate that it is possible to build the **SMD** as a pad multiwire chamber which will have an acceptable cost.

5 Acknowledgements

The authors are grateful for support by the Russian Fundamental Science Foundation under grant 95-02-05061 and the RHIC Department at BNL under contract 776746.

References

[1] Design and study of light readout system for scintillator shower maximum detector for EMC endcap. STAR Note 226.

[2] S.A.Akimenko et al. IHEP Preprint 94-94, Serpukhov,1994.

[3] J.Grunhaus, S.Kananov and C.Milstene, Nucl.Instr.and Meth. A354 (1995) 368-375

[4] C.Beard et al. Nucl.Instr. and Meth. A286(1990) 117-127

[5] L.Nodulman. Nucl.Instr. and Meth. 176(1980) 345-347
L.Balka et al. Nucl.Instr. and Meth. A267(1988) 272-279

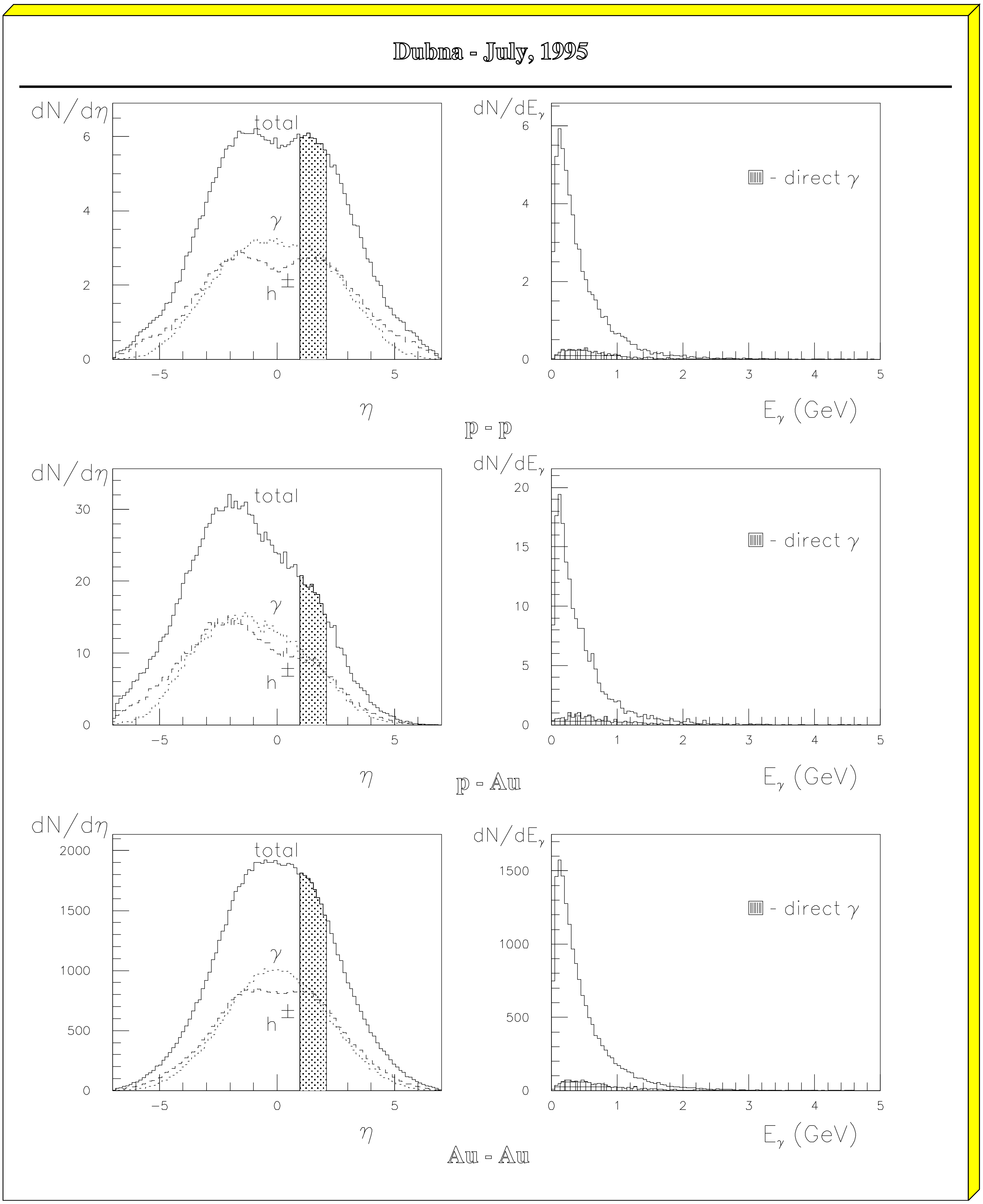

Figure 1: The pseudorapidity distribution of γ's and charged hadrons in **pp**, **pAu** and **AuAu** collisions at 200 Gev/nucleon

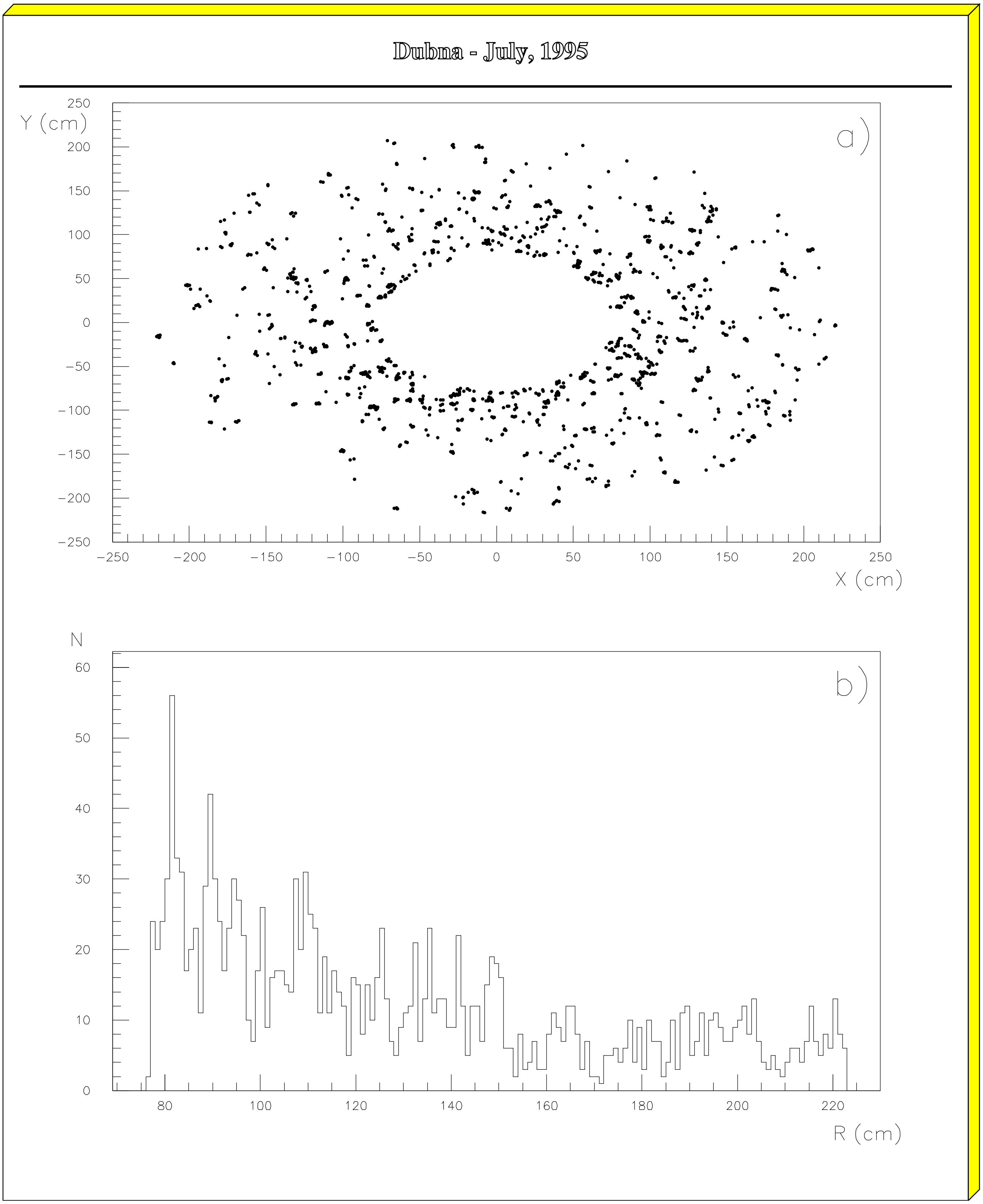

Figure 2: **(a)** Scatter plot of shower charged particles distribution on the first **SMD** layer; **(b)** The number of shower charge particle vs the distance from the **SMD** centre

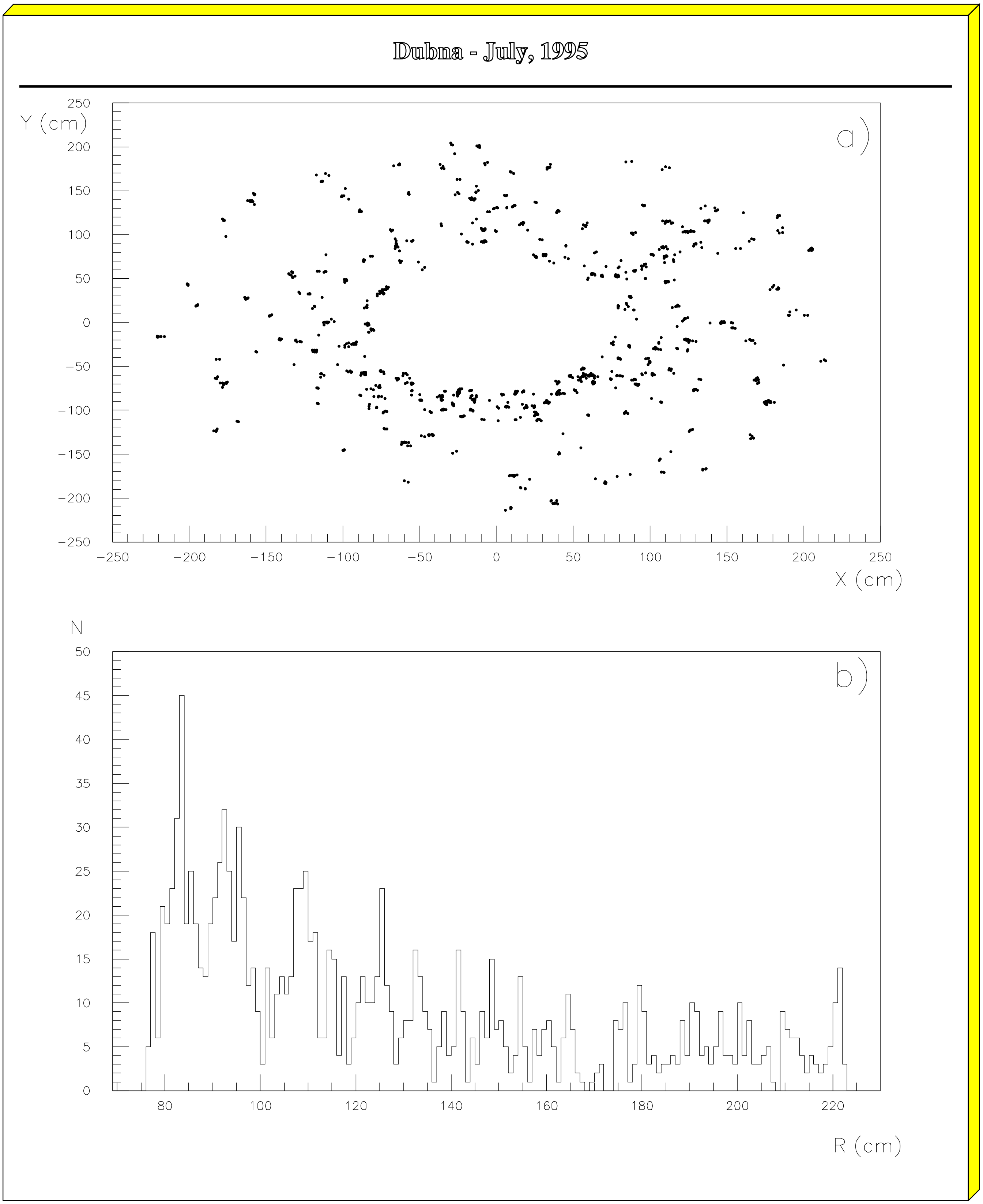

Figure 3: The same as **Fig.2** for the primary γ's with energy above 500 MeV

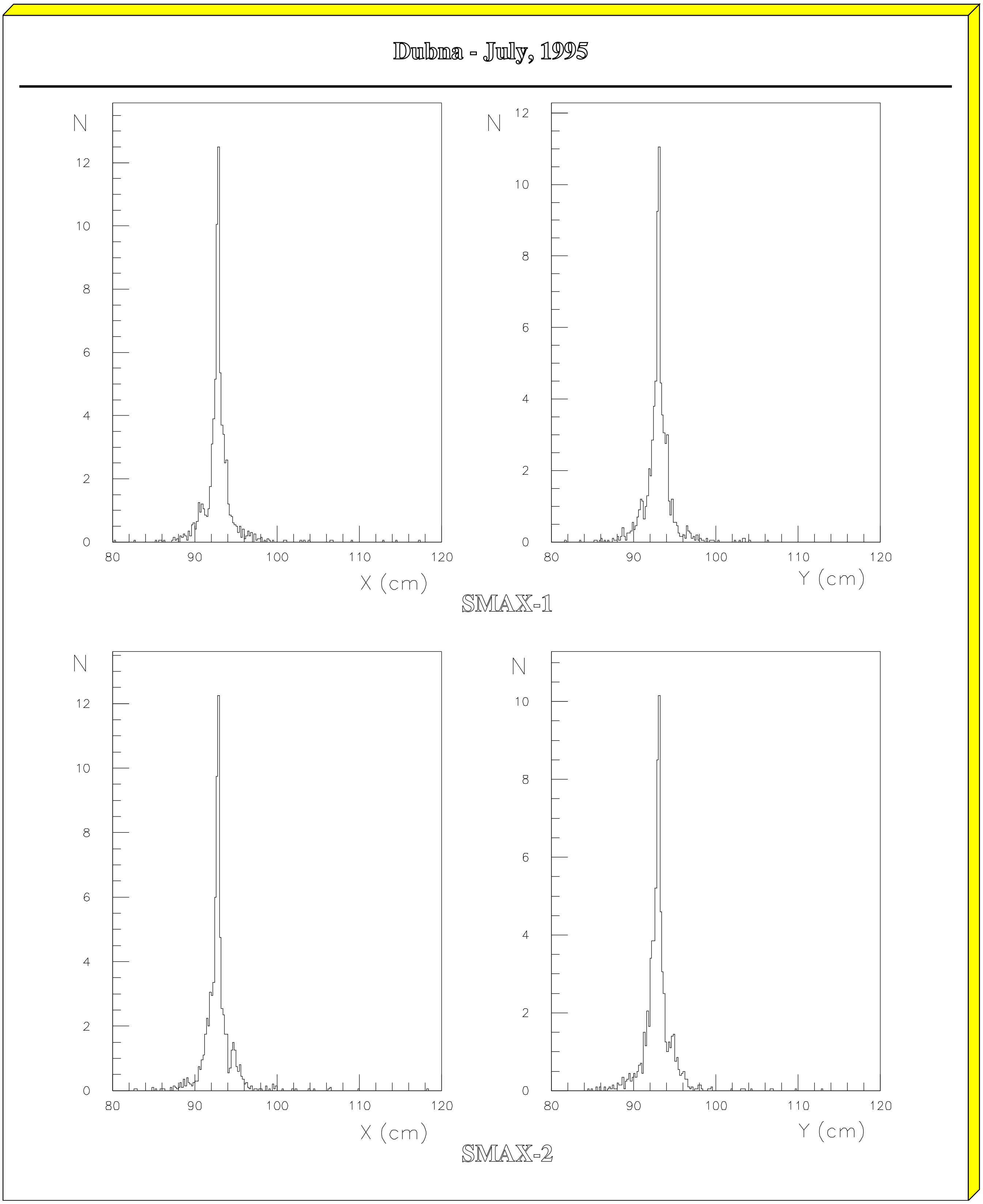

Figure 4: The transverse profiles of shower, induced by 15 GeV gamma

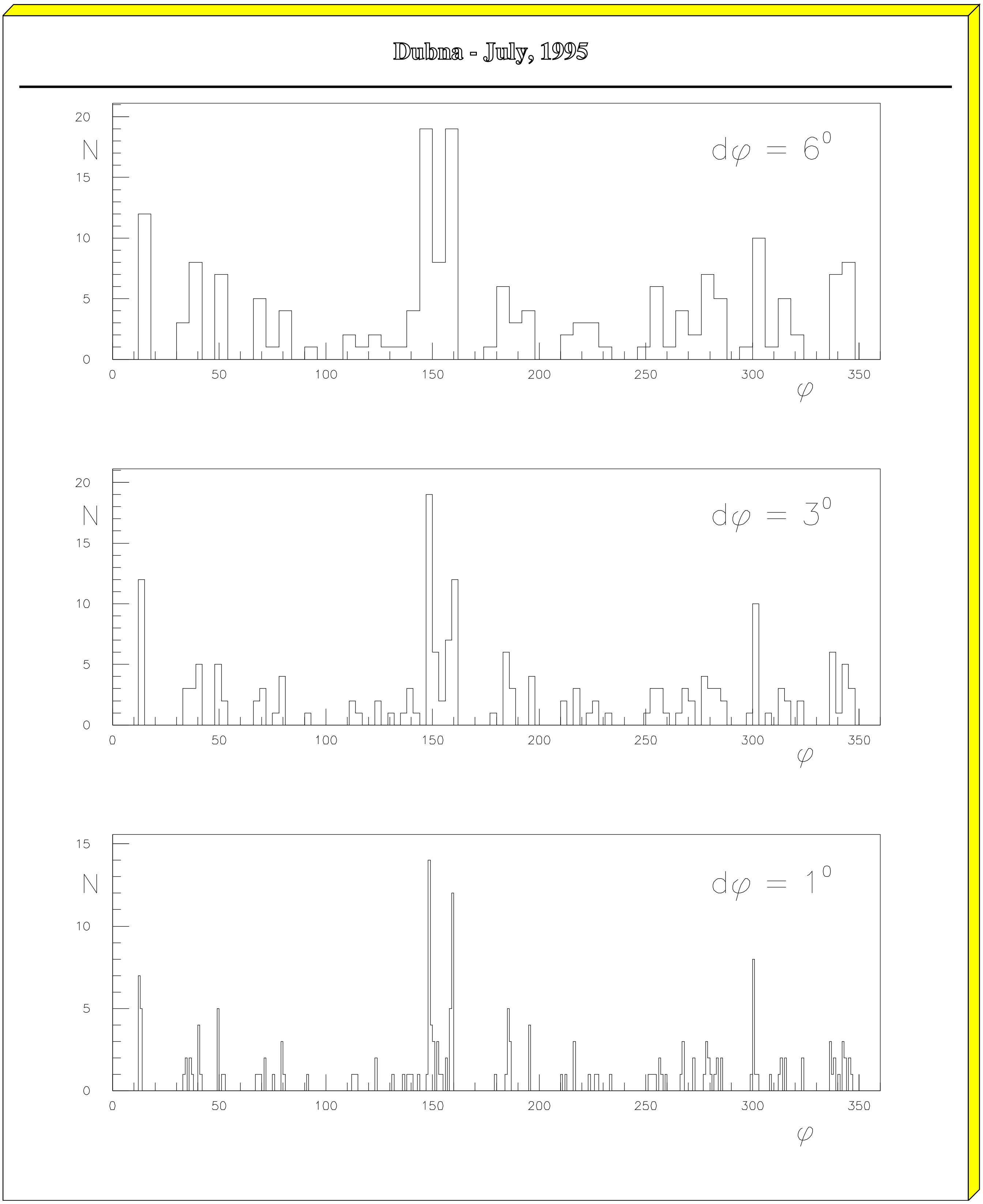

Figure 5: The energy deposited in the central 6 cm width ring of **SMD** vs. asimuthal angle for 6^o, 3^o and 1^o per bin for the central **AuAu** collisions

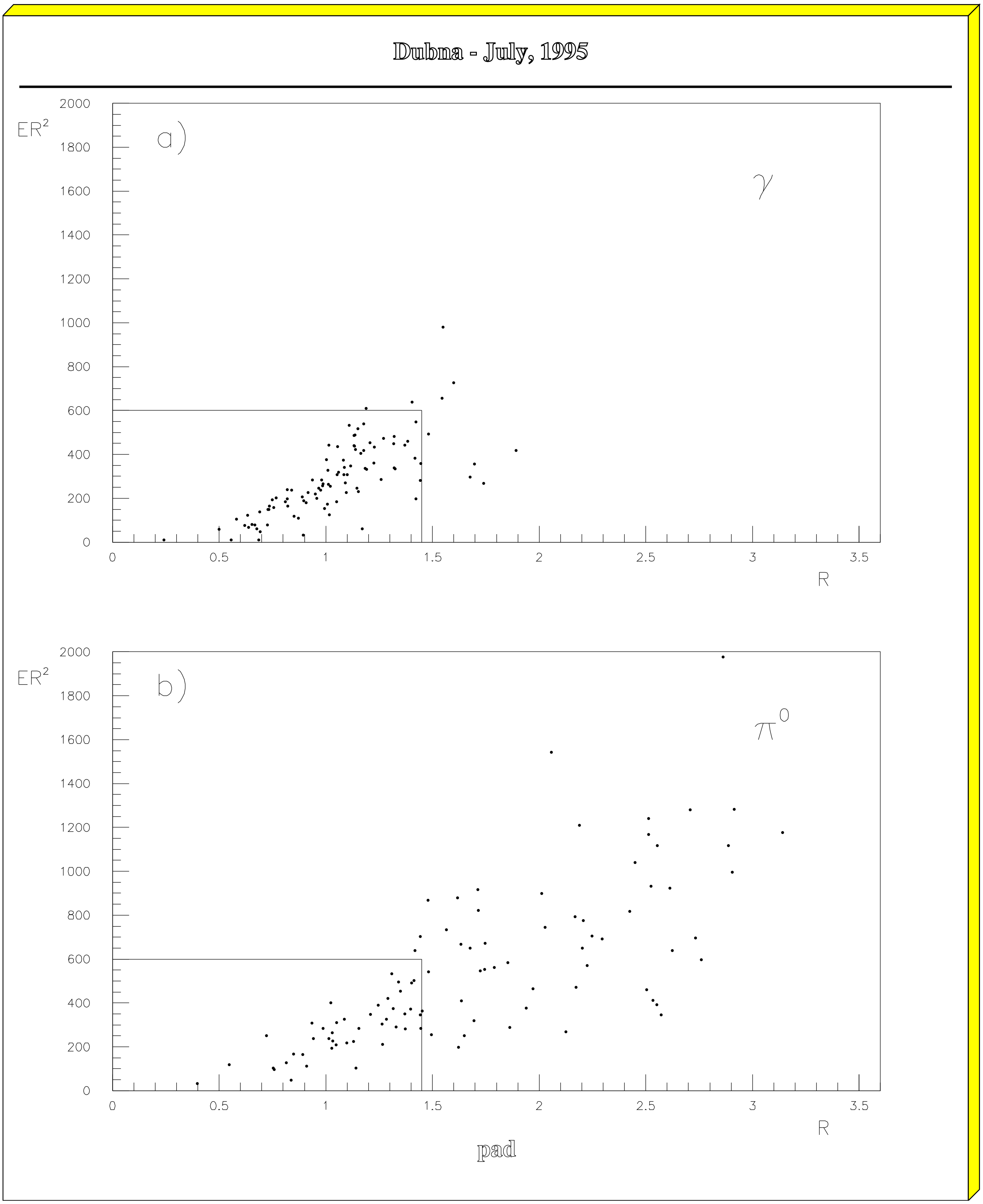

Figure 6: The scatter plot of sample of 15 GeV γ initiated showers as a function of the energy dispersion Er^2 and the weighted shower radius **r** for the **SMD** with one pad sensitive layer

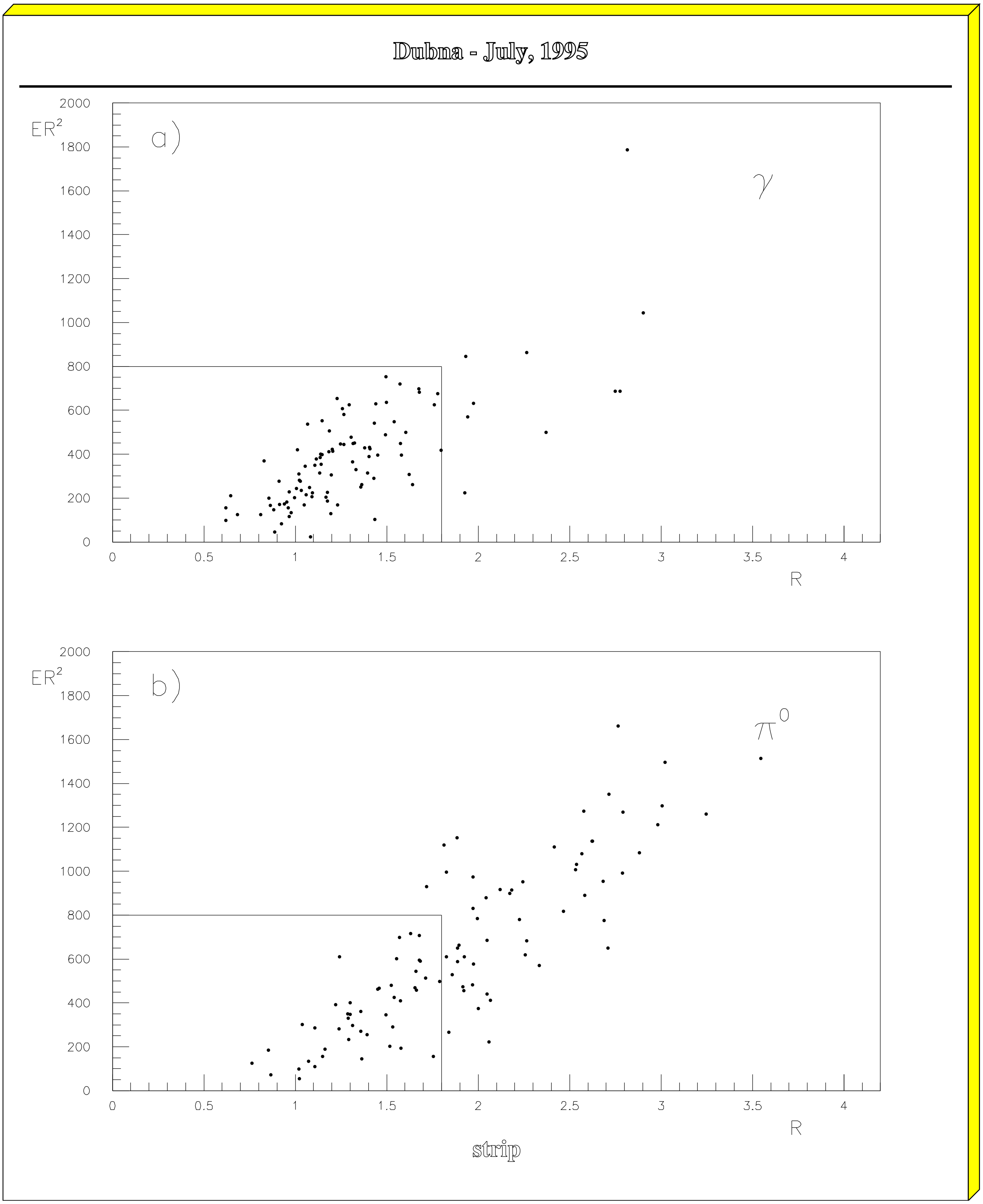

Figure 7: The same as in **Fig.6** for the **SMD** with two strip sensitive layer

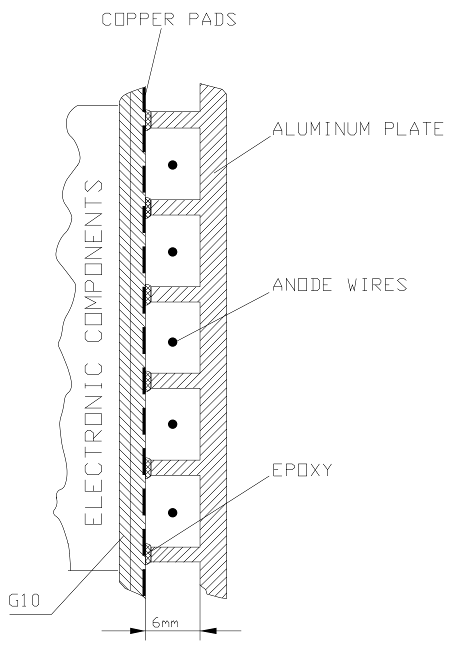

Figure 8: Layout and dimensions of the **SMD** multiwire gas chamber

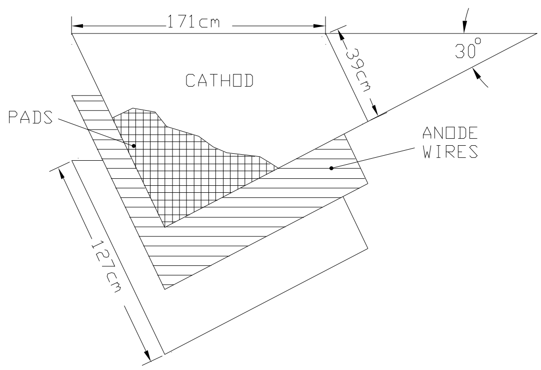

Figure 9: Schematic view of cross section of the **OPAL** type **SMD** multiwire gas chamber

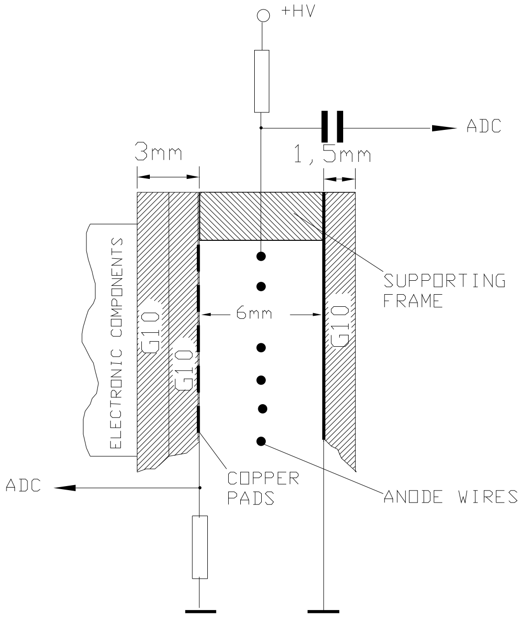

Figure 10: The same as in **Fig.9** for the **CDF** type chamber